

# Changes in extreme precipitation patterns over the Greater Antilles and teleconnection with large-scale sea surface temperature

Deleted: greater

Deleted: Caribbean

Carlo Destouches<sup>1,2</sup>, Arona Diedhiou<sup>2</sup>, Sandrine Anquetin<sup>2</sup>, Benoit Hingray<sup>2</sup>, Armand Pierre<sup>1</sup>, Dominique Boisson<sup>1</sup>  
Adermus Joseph<sup>1</sup>

Formatted: English (US)

<sup>1</sup>Universite d'Etat d'Haïti, Faculté des Sciences, LMI CARIBACT, URGéo, Port-au-Prince, Haïti

<sup>2</sup> Univ. Grenoble Alpes, IRD, CNRS, Grenoble INP, IGE, F-38000 Grenoble, France

*Correspondence to:* Carlo Destouches(carlo.destouches@univ-grenoble-alpes.fr)

## Abstract:

This study examines changes in extreme precipitation over the Greater Antilles, and their correlation with large-scale sea surface temperature (SST) for the period 1985 to 2015. The data used for this study were derived from two satellite products: Climate Hazards Group InfraRed Precipitation (CHIRPS) and NOAA DOISST (Daily Optimum Interpolation Sea Surface Temperature version 2.1) with resolutions of 5 km and 25 km, respectively. Then, change in the characteristics of six(6) extreme precipitation indices defined by the WMO ETCCDI (World Meteorological Organization Expert Team on Climate Change Detection and Indices) is analyzed, and Spearman's correlation coefficient has been used and evaluated by t-test to investigate the influence of a few large-scale SST indices: (i) Caribbean Sea Surface Temperature (SST-CAR); (ii) Tropical South Atlantic (TSA); (iii) Southern Oscillation Index (SOI); (iv) North Atlantic, Oscillation Index (NAO). The results show that at the regional scale, +NAO contributes significantly to a decrease in heavy precipitation (R95p), daily precipitation intensity (SDII), and total precipitation (PRCPTOT), whereas +TSA is associated with a significant increase in daily precipitation intensity (SDII). At an island scale, in Puerto Rico and southern Cuba, the positive phase of +TSA, +SOI, and +SST-CAR is associated with an increase in daily precipitation intensity (SDII) and heavy precipitation (R95p). However, in Jamaica and northern Haiti, the positive phases of +SST-CAR and +TSA are also associated with increased indices (SDII, R95p). In addition, the SST warming of the Caribbean Sea surface temperature and the positive phase of the Southern Oscillation (+SOI) is associated with a significant increase in the number of rainy days (RR1) and the maximum duration of consecutive rainy days (CWD) over the Dominican Republic and in southern Haiti.

Deleted: greater

Deleted: Caribbean

Deleted: ern

Deleted: ly

Deleted: s

Deleted: with

**Keywords:** Caribbean region; Greater Caribbean; Extreme precipitation; Climate variability; Sea surface temperature

Deleted: ¶

Deleted: ¶

48 **1 Introduction**

49 Over the past three decades, the climatic hazards to which the Caribbean Basin has been exposed include recurrent  
50 cyclonic and hydrometeorological hazards, characterized by increasing intensities (Joseph, 2006). The economic cost  
51 of 250 storms and floods over ~~40 years~~, (1970 to 2009) for 12 Caribbean countries amounted to US\$19.7 billion in  
52 2010, representing an annual average of 1% of gross domestic product (GDP) (Burgess et al., 2018). The most dreadful  
53 damage caused by these hydroclimatic events includes George in 1998, with 1,000 victims in the Dominican Republic  
54 and losses estimated at 14% of GDP, equivalent to approximately half the exports made that year (Naciones Unidas,  
55 Comision ~~Economica~~, para America ~~Latina~~, y el Caribe, 1988); Matthew in Haiti (October 2016), with over 500 dead,  
56 128 missing, 439 injured and 2.1 million people affected, including 895,000 children (De Giogi et al., 2021). Also,  
57 Hurricane Dorian caused property damage estimated at 2.5 billion USD when it came to rest over the Bahamas as a  
58 Category 5 storm in September 2019, rendering nearly 3,000 homes uninhabitable and causing extensive damage to  
59 hospitals, schools, and fisheries (Panamerican Health Organisation, 2019). A severe drought episode affected the  
60 island of ~~the~~ Caribbean from October 2019 to mid-2020, causing water shortages, bushfires, and agricultural losses.  
61 In Saint Vincent and the Grenadines, the 2020 drought was considered the worst of the 50 years (Nurse, 2020). The  
62 Inter-American Development Bank predicts that the Caribbean could face climate-related losses of over \$22 billion  
63 per year by 2050 (Inter-American Development Bank, 2014).

Deleted: a 40-year period

Deleted: economica

Deleted: Latima

Deleted:

Formatted: English (US)

64 In response to the climate extremes that are further weakening the island states of the Caribbean region, already in a  
65 situation of extreme socio-economic precariousness, several studies have been carried out in parallel to understand  
66 the associated physical processes and anticipate the evolution of these extreme climatic ~~events~~. Research into the  
67 Caribbean climate goes back to the second half of the twentieth century and has focused mainly on rainfall patterns  
68 (Curtis et al., 2008), as well as on the overall description of rainy seasons (Griffiths et al., 1982).

Deleted: events

69 A more detailed study of the climate of the Caribbean was performed in 2001 and 2002 using indices derived from  
70 daily data to detect climate change (Peterson et al., 2001; Frich et al., 2002). This approach, which uses indices defined  
71 by the World Meteorological Organization's group of experts to characterize precipitation and temperature extremes,  
72 has enabled several studies to examine the state of climate extremes over the Caribbean (Stephenson et al., 2014;  
73 McLean et al., 2015). The results of these previous assessments agree that the frequency and intensity of climate  
74 extremes (~~heavy rainfall, drought spell, wet spell~~) over the Caribbean have increased over the last 30 years (Stephenson  
75 et al., 2014; Peterson et al., 2002a; Beharry et al., 2015; Dookie et al., 2019), ~~and will continue to do so until the end~~  
76 of the century (Taylor et al., 2018; Vichot-Llano et al., 2021; Hall et al., 2013; Almazroui et al., 2021; McLean et al.,  
77 2015).

Formatted: Font color: Text 1

Formatted: Font color: Text 1

78 Climate teleconnections, the remote forcing of a region far from the source of disturbance, whether simultaneous or  
79 time-lagged (Mariami et al., 2018; Rodrigues et al., 2021), are generally derived from variations in sea surface  
80 temperature (SST) or atmospheric pressure at seasonal to interdecadal scales. Several of these have been shown to  
81 play a major role in modifying global weather patterns (Hurrell et al., 1995; Martens et al., 2018).

Deleted: ¶

87 Previous studies have also shown the effect of east-west gradients in SST anomalies in the tropical Pacific and Atlantic  
88 on precipitation in the Caribbean, with a tendency for a warm Atlantic and a cold Pacific to favor precipitation in the  
89 Caribbean (Taylor et al., 2002a; Gimeno et al., 2011). Studies (Enfiel et al., 2001; IPCC, 2007) also found that the  
90 monthly ~~AMO (Atlantic Multidecadal Oscillation)~~ index is an SST signal in the North Atlantic that influences the  
91 decadal-scale variability in precipitation. In addition, Peterson et al. (2022) analyzed the link between SST,  
92 temperature, and precipitation extremes over the Caribbean using ground-based observations. They showed that the  
93 extreme precipitation index (SDII) averaged over the Caribbean has a strong correlation with SST over the Caribbean  
94 and the entire tropical North Atlantic Ocean. The work of Stephenson et al. (2014) examined the influence of the  
95 Atlantic Multidecadal Oscillation (AMO) on extreme precipitation from a ground-based observation network in the  
96 Caribbean. These results show that the AMO influences the variability of extreme temperature and precipitation  
97 events. ~~However, considering that the effects of teleconnections caused by large-scale SSTs on weather are expected  
98 to become more extreme in the future due to climate change (Mariami et al., 2018), further research is needed on other  
99 SST indices such as NAO, SOI, TSA, SST-Car, for which no in-depth studies have been carried out.~~

100 In this context, ~~this study aimed~~ to examine the remote impact of the tropical Pacific Ocean, Atlantic Ocean, and the  
101 Caribbean Sea on observed changes in the tropical islands of the Greater Antilles, particularly the links between  
102 extreme precipitation indices and large-scale sea surface temperature indices. This paper is organized into five  
103 sections: Section 1 presents the study area and the associated climatology. Sections 2 and 3 describe the spatio-  
104 temporal variability of extreme precipitation indices at regional and local scales and the influence of SST indices on  
105 extreme precipitation. The last sections (4-5) present the discussion and conclusion.

106

## 107 2 Study Area and Data

### 108 2.1 Study area

109 The Greater Antilles is a region between North and South America made up of four islands bordered by the Caribbean  
110 Sea to the south and the Atlantic Ocean to the east (Fig.1). These islands include Cuba, Hispaniola, Jamaica, and  
111 Puerto Rico. They have a monthly rainfall cycle characterized by two peaks: the first in May and the second between  
112 September and October (Giamini et al., 2000). The climatology of monthly rainfall in the Greater Antilles is strongly  
113 influenced by the subtropical North Atlantic anticyclone (Davis et al., 1997), low-level jet (CLLJ), characterized by  
114 two peaks: the first in January and the second in July (Cook and Vizy, 2010). This jet plays a key role in transporting  
115 moisture to the Caribbean (Mo et al., 2005). They were also influenced by the intertropical convergence zone (ITCZ)  
116 (Hastenrath, 2002), with maximum precipitation in May (sup.fig.1b). Heavy autumn rainfall in the Greater Antilles  
117 (supl.fig.1d) is generally associated with North Atlantic tropical cyclones, 85% of which are of high intensity and  
118 originate from African easterlies (Agudelo et al., 2011; Thorncroft and Hoge, 2001) under warm Atlantic basin  
119 conditions. The spatial distribution of the total annual precipitation in the Greater Antilles, particularly on the islands,  
120 is not homogeneous due to the complexity of topography (Moron et al., 2015, Cantet, 2007). Precipitation is relatively

Deleted: in

Deleted: AMO

Deleted: (

Deleted: et al.

Deleted: ,

Deleted: )

Deleted: air

Deleted: (

Deleted: et al.

Deleted: ,

Deleted: ;

Deleted: however, further research is needed. In addition, the effects of teleconnections caused by large-scale SST on weather conditions are expected to become more extreme in the future due to climate change (Mariami et al., 2018).

Deleted: the aim of this study was

Deleted: area

Deleted: peaks:

Deleted: November

Deleted:

Deleted: the easterly winds of the intertropical zone, and the trade winds (Cook et al., 2010).

Deleted:

Deleted: et al.,

Deleted: 2

Deleted: et al.

Deleted: . The total annual precipitation in the Greater Antilles depends on land-sea interactions (breezes) and topography (fig.1a)

Deleted: because

Deleted: , 2015

Deleted: ¶

152 high (2,000-24,000< mm/year) at higher altitudes and in wind-exposed areas (supl.fig.1b). In contrast, annual  
153 precipitation can reach 500 mm/year in leeward areas (Daly et al., 2003).

154  
155 **2.2 Satellite data**

156 This study was conducted using two satellite datasets: NOAA DOISST Sea surface temperature data and CHIRPSv2  
157 data. The CHIRPSv2 data (Climate Hazards Group Infrared Precipitation with Stations data version 2) are quasi-  
158 global daily precipitation data (50S-50N) with a resolution of 0.050, available over a period from 1981 to 2022(Funk  
159 et al., 2015). Based on the techniques used by NOAA for estimating precipitation in the thermal infrared (Love et al.,  
160 2004), the CHIRPSv2 database was built from precipitation estimates based on cold cloud duration observations, and  
161 a fusion incorporating monthly CHPClim (Funk et al., 2015a) (Climate Hazards Group Precipitation Climatology  
162 (CHPClim) precipitation data, and in situ data from ground observation networks. TRMM 3B42v7 (Tropical Rainfall  
163 Measuring Mission Multi-Satellite Precipitation Analysis) satellite products were also used to calibrate and reduce the  
164 bias in the estimates. The results of global and regional validation studies showed that CHIRPSv2 can be used to  
165 quantify the hydrological impacts of decreasing rainfall and increasing air temperatures in the Greater Horn of Africa  
166 (Funk et al., 2015). In addition, the performance of CHIRPSv2, evaluated over certain regions of the Americas, has  
167 demonstrated its ability to reproduce the mean climate as well as its capacity to estimate extreme precipitation events  
168 (Rivera et al., 2019). Furthermore, in Colombia, the best results were obtained on a daily and monthly scale over the  
169 Magdalena River Basin (Baez-Villanueva et al., 2018). CHIRPSv2 data are suitable for our study, as they perform  
170 well in the Caribbean (Centella-Artolla et al., 2020), and in the study by Bathelemy et al.(2022), it was shown that Chips  
171 perform well in estimating heavy precipitation based on the 90<sup>th</sup> percentile(Bathelemy et al., 2022).

172 Sea surface temperatures (SST) are very important for monitoring and assessing climate change (IPCC, 2013). They  
173 can be derived either from observations from floating or moored buoys (Smith et al., 1996), from satellite observations  
174 (Merchant et al., 2014), or from a mixture (in situ + satellite) (HadSST, Rayner et al., 2003) and (DOSST, Reynold et  
175 al., 2007). In this study, NOAA DOISST (Daily Optimum Interpolation Sea Surface Temperature version 2.1) data  
176 were used; these are also daily sea surface temperature data derived from a combination of in situ sea surface  
177 temperature (SST) data obtained from ships and buoys and sea surface temperatures obtained from the Advanced Very  
178 High-Resolution Radiometer (AVHRR)(Reynold et al., 2007; Huang et al., 2021). This satellite product is the result  
179 of a global file of 0.250-degree grid points, available over the period 1981-2020. In addition, it has been widely used  
180 for climate assessment and monitoring, notably as part of the reanalysis of the NOAA/NCEP climate prediction system  
181 (Saha et al., 2010). Work by Huang et al.(2021a) has revealed that NOAA DOISST performs well in terms of bias  
182 compared with buoy and Argo observations, as well as with the eight SST products.

183  
184

Deleted: ¶

Deleted: events

Deleted: or example

Deleted: (the largest in Colombia)

Deleted: CHIRPS data are suitable for our study, as their performance over the Caribbean, particularly the Greater Antilles, has shown their ability to estimate heavy precipitation (Bathelemy et al., 2022).

Formatted: Superscript

Deleted: are

Deleted: High Resolution

Deleted: )

Deleted: ¶

Deleted: ¶

197 **3. Methodology**

198 The World Meteorological Organization's Expert Team on Climate Change Detection and Indices (ETCCDI) has  
199 defined 27 indices to characterize extreme precipitation and temperature events in terms of frequency, amplitude, and  
200 duration (Peterson et al., 2001). Although the proposed method includes numerous indices based on percentiles, with  
201 thresholds set to assess extremes that generally occur a few times a year and not necessarily high-impact events, it has  
202 paved the way for numerous research projects in the Caribbean (Stephenson et al., 2014; McLean et al., 2015). Six  
203 extreme precipitation indices (see Table 1 for details) were calculated: total annual precipitation (PRCPTOT), number  
204 of rainy days (RR1), intensity of rain events (SDII), and heavy precipitation (R95p), calculated with a threshold  
205 corresponding to the 95th percentile of the daily precipitation distribution, maximum number of consecutive wet days  
206 (CWD), and maximum number of consecutive dry days (CDD).

207 The spatiotemporal evolution of extreme precipitation in the Greater Antilles was investigated by analyzing the  
208 interannual variability of extreme precipitation index anomalies over a long period (1985-2015) and the change in  
209 percentage variations in extreme precipitation indices at decadal timescales. To characterize the percentage variations,  
210 we chose the (Pij) index, which is already used in the study by An et al. (2023), whose equation is presented hereafter.

211 
$$P_{ij} = \left( \frac{P_{i(j+1)}}{P_{ij}} - 1 \right) \times 100 \quad (1)$$

212 Where Pij is the average extreme precipitation index for the j-th decade at the i-th location, and Pi(j+1) is the average  
213 extreme precipitation index for the (j+1)-th decade at the i-th location.

214 Previous studies have shown that precipitation in the Caribbean, particularly in the Greater Antilles, is influenced by  
215 the surface temperature of the Atlantic Ocean and tropical Pacific (Gimeno et al., 2011; Enfiel et al., 2001). Thus, to  
216 investigate the impact of these basins on extreme precipitation over indices, we selected four large-scale SST indices,  
217 namely the Southern Oscillation Index (SOI), the North Atlantic Oscillation (NAO) (Jones et al., 1997), the Tropical  
218 South Atlantic Anomaly Index (TSA) and the Caribbean Sea Surface Temperature Anomaly Index (SST-CAR).  
219 Details of these indices can be consulted online; <https://psl.noaa.gov/data/climateindices/list/#Nina34>.

220 Analysis of the relationship between two variables is often of great interest for data analysis in research. It generally  
221 consists in characterizing the form and intensity of the link (relationship) between variables using a correlation  
222 coefficient. For two variables, X and Y, this coefficient is interpreted as: i) linear linkage, the correlation coefficient is  
223 positive when X and Y values change in the same direction, that is, an increase in X leads to an increase in Y; ii) linear  
224 linkage, the correlation coefficient is negative when X and Y values change in the opposite direction, that is, an  
225 increase in X leads to a decrease in Y (or vice versa); iii) non-linear monotonic linkage, the correlation coefficient is  
226 positive when X and Y change in the same direction as in (i), but with a small slope (Lewis-Beck, 1995; Sheskin,  
227 2007).

**Deleted:** To provide countries with information on extreme weather events, a group of World Meteorological Organization experts (ETCCDI: Expert Team on Climate Change Detection and Indices) defined 27 indices to characterize extreme precipitation and temperature events in terms of their frequency, amplitude, and duration (Peterson et al., 2001)

**Deleted:** (6)

**Deleted:** Table 1

**Deleted:** in relation to

**Deleted:** (

**Deleted:** et al.

**Deleted:** ,

**Formatted:** English (US)

**Deleted:** where

**Formatted:** English (US)

**Deleted:** Then, as the variability of precipitation in the region is known to be linked to SST in the tropical Pacific and Atlantic (Gimeno et al., 2011; Enfiel et al., 2001), we selected four large-scale SST indices, namely the Southern Oscillation Index (SOI), the North Atlantic Oscillation (NAO) (Jones et al., 1997), the Tropical South Atlantic Anomaly Index (TSA), and the SST over the Caribbean Sea (SST-CAR), and investigated the teleconnection between these indices and the precipitation extremes in the region. Detailed descriptions and estimates of these SST indices are available in (<https://psl.noaa.gov/data/climateindices/list/#Nina34>).

**Formatted:** c-pjlv, Font: 10 pt, English (US)

**Formatted:** Hyperlink, Font: 10 pt, English (US)

**Formatted:** Font: 12 pt

**Field Code Changed**

**Formatted:** Justified, Line spacing: 1,5 lines

**Deleted:** ¶

253 In the literature, Pearson's and Spearman's correlation coefficients are often the most widely used to measure the  
 254 strength or degree of linkage between two variables. In this study, we used Spearman's non-parametric rank correlation  
 255 coefficient (rho) to assess the interannual link between extreme precipitation over indices and global SSTs indices.  
 256 This non-parametric method was chosen because it does not require a normal distribution for the variables. Also,  
 257 Spearman outperforms Pearson's linear coefficient in the case of outliers. On the other hand, linear trends can be  
 258 detected using Pearson or Spearman tests, but the latter is preferable for monotonic non-linear relationships (Gauthier,  
 259 2001; Von Storch and Zwiers, 1999). Spearman's correlation has already been used in several studies to assess the  
 260 links between teleconnection patterns and precipitation. (Rios-Cornejo et al., 2015; Khadgarai et al., 2021).

261 Spearman's correlation coefficient is calculated using the following equation:

$$r_{\text{spearman}} = \frac{\sum_{i=1}^n (R_i - R)(S_i - S)}{\sqrt{\sum_{i=1}^n (R_i - R)^2 \sum_{i=1}^n (S_i - S)^2}} \quad (2)$$

263 Where, r spearman is the correlation coefficient, Ri=rang (Xi), Si=rang (Yi) are respectively the data ranks of  
 264 Variables X and Y (X: Extreme precipitation index, Y: Large-scale SST index).

265 To test the significance of the relationship, whether the two variables are correlated or not, we use the t-test for a  
 266 threshold of 0.05 or less. This involves testing the two hypotheses (H<sub>0</sub> and H<sub>1</sub>) based on the value of t to deduce the  
 267 probability of observing a result that deviates as much as expected from the correlation. The formula for calculating  
 268 the value of t using Spearman's correlation is as follows:

$$t_{n-2} = \frac{r_{\text{spearman}}}{\sqrt{\frac{1-r_{\text{spearman}}^2}{n-2}}} \sqrt{n-2} \quad (3)$$

270 Where:

271 n-2: degrees of freedom.  
 272 n: sample size

## 274 4 Results

### 275 4.1 Changes in precipitation extreme indices

276 Interannual changes in extreme precipitation indices over the Greater Antilles are shown in Fig. 2. As shown in Fig.  
 277 2a, the period from 1985 to 1994 was generally marked by a decline in total annual precipitation. This decline was  
 278 associated with a decrease in average rainfall intensity (Fig. 2c) and a reduction in the length of wet and dry spells  
 279 (Fig. 2e, 2f). On the other hand, the period from 1995 to 2004 was mainly characterized by a decrease in the number  
 280 of rainy days (fig.2b), associated with an increase in the average intensity of precipitation (fig. 2c) and in the  
 281 contribution of heavy precipitation (fig. 2d). Furthermore, during the period 2005-2015, an increase in the contribution  
 282 of heavy precipitation was observed until 2012(fig.2d). This was associated with an increase in the number of rainy  
 283 days(fig.2b), an increase in the average intensity of precipitation(fig.2c) and in the length of wet episodes(fig.2e).

- Deleted: The teleconnection between SST and extreme (... [1])
- Deleted: Such an analysis with
- Deleted: Spearman correlation has already been carried (... [2])
- Formatted (... [3])
- Deleted: Chen et al., 2015; Sunilkumar et al., 2016
- Formatted (... [4])
- Deleted: . This coefficient was interpreted over a close (... [5])
- Formatted (... [6])
- Formatted (... [7])
- Formatted (... [8])
- Formatted (... [9])
- Formatted (... [10])
- Formatted (... [11])
- Formatted (... [12])
- Formatted (... [13])
- Formatted (... [14])
- Formatted (... [15])
- Formatted (... [16])
- Formatted (... [17])
- Formatted (... [18])
- Formatted (... [19])
- Formatted (... [20])
- Formatted (... [21])
- Formatted (... [22])
- Formatted (... [23])
- Formatted (... [24])
- Formatted (... [25])
- Deleted: where
- Deleted: that is,
- Deleted: really
- Deleted: 0
- Formatted (... [26])
- Formatted (... [27])
- Formatted (... [28])
- Formatted (... [29])
- Formatted (... [30])
- Formatted (... [31])
- Formatted (... [32])
- Deleted: ¶
- Formatted (... [33])
- Formatted (... [34])
- Formatted (... [35])
- Deleted: ¶

307

308 Fig. 3 shows the annual change in percentage between two consecutive decades of precipitation indices over the  
 309 Greater Antilles (1985-2015). As shown in fig. 3(a, d2), there was an increase in total annual precipitation  
 310 (PRCPTOT) in southeastern Cuba. This was associated with an increase in the number of rainy days (RR1) (fig.3(b,  
 311 d2)) and the average intensity of precipitation per rainy day (SDII) (fig.3(c, d2)). These results were also observed in  
 312 Puerto Rico, with an increase in total annual precipitation associated with an increase in RR1 (fig.3(a, d2), 3(b, d2)).  
 313 In addition, a decrease in total annual precipitation (PRCPTOT) was observed on the island of Hispaniola (Dominican  
 314 Republic and Haiti, except for the southern part) (fig.3(a, d2)). This was associated with a decrease in the average  
 315 rainfall intensity per wet day (SDII) (fig.3(c, d1)). This decrease in the SDII was also recorded in Puerto Rico (fig.3(e,  
 316 d2)). For heavy precipitation (R95p), as shown in fig.3(d, d2), an increase was observed in the southeastern part of  
 317 Cuba, whereas the whole island (Cuba) was affected in general by a decrease in wet sequences (CWD) (fig.3(e, d2))  
 318 and dry sequences (CDD) (fig.3(f, d2)). A decrease in heavy precipitation (R95p) was observed in the central and  
 319 western regions of Haiti (fig.3(d, d2)). This was accompanied by an increase in wet sequences (CWD) over Haiti  
 320 (fig.3(e, d2)). The Dominican Republic was also affected by this increase in wet sequences (CWD) (fig.3(e, d2)).

321 Variations in extreme precipitation indices under the influence of variables such as NAO, SOI, TSA, and SST-CAR  
 322 were analyzed over the Greater Antilles. The influences of large-scale variables were classified as positive, negative,  
 323 positive, significant, negative, or significant, as shown in figure 4. The results obtained by taking the intersections of  
 324 the table in fig. 4, presented show the values of the correlation coefficient (with its significance \*) between the extreme  
 325 precipitation indices (PRCPTOT, RR1, SDII, R95p, CWD, and CDD) and the influencing variables (NAO, SOI, TSA,  
 326 and SST-CAR). Thus, the table in fig. 4 shows that NAO has a negative effect on all extremes, while the other SST-  
 327 CAR are positive, except for the number of rainy days (RR1) and the number of consecutive rainy days (CWD).  
 328 However, the positive phase of the +TSA index had a positive and significant effect on the average rainfall intensity  
 329 per wet day (SDII), for which a correlation coefficient of 0.37 was obtained. Similarly, with the ONA index, a negative  
 330 and significant effect (P<0.05) was observed on total annual precipitation (PRCPTOT), average precipitation intensity  
 331 (SDII), and heavy precipitation (R95p), for which correlation coefficients of 0.49, 0.40, and 0.47, respectively, were  
 332 obtained.

333 At a local scale, the results show that teleconnections have had positive and significant effects on extreme precipitation  
 334 indices over the last 30 years in the countries of the Caribbean region, particularly in the Greater Antilles. The spatial  
 335 extent of significance is indicated by the symbols (\*). Thus, the double symbol (\*\*) represents regions with a  
 336 significant surface area greater than 50% of the surface area, while the symbol (\*) is used for a significant surface area  
 337 less than 50%. The figures (with a threshold at  $p \leq 0.05$ ; fig. 5, 6, 7, 8) show the regions or countries over which  
 338 positive and significant effects were observed for the Greater Antilles.

339 Fig. 5 and suppl. Table 1 shows the effect of the TSA index on extreme precipitation indices (PRCPTOT, RR1, SDII,  
 340 R95p, CWD, and CDD) in the Greater Antilles. The results show that South Atlantic tropical warming, corresponding

**Deleted:** The observed changes in total annual precipitation (PRCPTOT), number of rainy days (RR1), rainfall intensity (SDII), contribution of heavy rainfall (R95p), and maximum duration of consecutive rainy days (CWD) and dry days (CDD) in the Greater Antilles over the three decades (1985-1994, 1995-2004, 2005-2015) are shown in fig. 2. The first decade of 1985-1994 was generally marked by a decline in total annual precipitation (fig.2a), associated with a decrease in the number of rainy days (fig. 2b), a decrease in the average rainfall intensity (fig. 2c), a decrease in the contribution of heavy rainfall (fig. 2d), and in the length of wet and dry spells (fig. 2e, 2f). The second decade 1995-2004, was mainly characterized by an increase in rainfall associated with an increase in rainfall intensity, the contribution of heavy rainfall, and the length of dry spells. The last decade 2005-2015, was characterized by a wet period (until 2012) followed by a dry period. Except for 2008-2009, the wet period was generally associated with positive anomalies of all indices, whereas the last dry period exhibited negative anomalies in all indices except during rainy days, which showed a weak change.¶

- Deleted: %
- Deleted: a
- Deleted: c
- Deleted: These results were also observed in Jamaica
- Deleted: c
- Deleted: Haiti and the Dominican Republic
- Deleted: c
- Deleted: f
- Deleted: s
- Deleted: T
- Deleted: s
- Deleted: show

**Deleted:** Thus, a double symbol (\*\*) indicates that the effect extends over a wide area, whereas the effect is limited to that bearing a single symbol (\*)

**Deleted:** P

**Deleted:** ¶

378 to the positive phase of the +TSA index, has a positive and significant effect (\*\*) on the total annual precipitation  
379 (PRCPTOT) and heavy precipitation (R95p) in Puerto Rico (fig.5a, 5b; suppl. table1d). In Jamaica, it was also  
380 associated with an increase in total annual precipitation (PRCPTOT) and heavy precipitation (R95p) (fig.5a, 5b;  
381 suppl. table1d). In Haiti, more specifically in the northern part, the increase in the average daily rainfall intensity  
382 (SDII) was also associated with +TSA warming (fig.5e; suppl. table1d). In northwest Cuba, this positive phase of  
383 +TSA also had a positive and significant effect (\*\*) on mean rainfall intensity per day (SDII) (fig.5e; suppl. table1d).  
384 Conversely, in southeastern Cuba, a positive effect was observed for heavy rainfall (R95p) (fig.5b; suppl. table1d).

Deleted: in Puerto Rico

385 Fig. 6 and suppl. Table 1a shows the effects of warming of the Caribbean Sea surface temperature (SST-Car anomaly,  
386 averaged over 14-16N, 65-85 °W) on extreme precipitation in the Greater Antilles. In southern Haiti, an increase in  
387 total annual precipitation (PRCPTOT) and the number of rainy days (RR1) was observed as the SST-Car warmed  
388 (fig.5a, 5c; suppl. table1a). In the same region, this increase was also observed for heavy rainfall (R95p) (fig.6b; Suppl.  
389 table1a). In eastern Haiti, particularly in Santo Domingo, the positive phase of + SST-Car is associated with an increase  
390 in the duration of wet sequences (CWD) and the number of rainy days (RR1) (fig.6c, 6d; suppl. table1a). In  
391 southeastern Cuba, especially on the Caribbean coast, warming of SST-Car is associated with an increase in total  
392 annual precipitation (PRCPTOT) and heavy precipitation (R95p) (fig.6a, 6b; suppl. table1a). An increase in heavy  
393 precipitation (R95p) during the positive phase of + SST-Car was also observed in Puerto Rico (fig.6c; Suppl. table1a).

Deleted: 2

Deleted: T

Deleted: c

Deleted: c

Deleted: Cuba

394 Fig. 7 and suppl. Table 1c shows the results of the effect of SOI on extreme precipitation indices (PRCPTOT, RR1,  
395 SDII, R95p, CWD, and CDD) in the Caribbean region, particularly on the islands forming the Greater Antilles. In  
396 Puerto Rico, as shown (fig.7a, 7b; suppl. table1c), the positive phase of the +SOI index was associated with an increase  
397 in total annual precipitation (PRCPTOT) and heavy precipitation (R95p). In Haiti, specifically in the south, this  
398 positive phase of the +SOI index was associated with an increase in the number of rainy days (RR1), including the  
399 duration of wet sequences (CWD) (fig.7c, 7d; suppl. table1c). In Santo Domingo, this is associated with an increase  
400 in the duration of wet sequences (CWD) (fig.7d; suppl. table1c). In southeastern Cuba, this is associated with an  
401 increase in the average intensity of precipitation per rainy day (SDII) and heavy precipitation (R95p) (fig.7e, 7b; suppl.  
402 table1c).

Deleted: table1

Deleted: show

Deleted: carab

Deleted: id beetles

403 Fig. 8 and suppl. Table 1b shows the results of the effect of the NAO index on extreme precipitation indices  
404 (PRCPTOT, RR1, SDII, R95p, CWD, and CDD) in the Greater Antilles. The condensed results for different phases  
405 of the NAO index are presented in Supplementary Table 1b. In contrast to the results for the other large-scale SST  
406 indices, the positive phase of the +NAO index was only associated with an increase in the number of rainy days (RR1)  
407 over Cuba. This increase was greater for coasts facing the Caribbean Sea (fig.8c; Suppl. Table).

Deleted: table1

Deleted: show

Deleted: ESS

Deleted: table1b

408

Deleted: ¶

409

410

Deleted: ¶

426

## 427 5. Discussion

428 The results of this study showed that extreme precipitation over the period 1985-2015 was influenced by four large-  
 429 scale sea surface temperature indices (NAO, SOI, TSA, SST-Car). On the other hand, on a local scale, notably over a  
 430 few regions, the effects of this influence on certain precipitation indices were statistically significant, while on other  
 431 precipitation indices, non-significant effects were observed. To shed more light on these results, we discuss the  
 432 following points: i) Impact of sea surface pressure anomalies (NAO, SOI); ii) Impact of sea surface temperature  
 433 anomalies (TSA, SST-Car).

### 434 5.1 Impact of sea surface pressure anomalies (NAO, SOI)

435 In this study, the influence of the Atlantic Ocean over the Greater Antilles is assessed using two large-scale SST  
 436 indices (NAO, Hurrell (2003)) and TSA. The phases (positive and negative) of the NAO index have been shown to  
 437 affect circulation in the Northern Hemisphere (Thompson et al., 2000). Also, this index is a measure of the meridional  
 438 pressure gradient between the NASH and the Icelandic low (Visbeck et al., 2001). Nevertheless, in this study, the  
 439 results show that the NAO has a negative effect on all extreme precipitation over indices in the region (fig.4). In other  
 440 words, the fluctuation of the NAO index and extreme precipitation over indices change in opposite phases, i.e. the  
 441 negative (or positive) phase of the NAO is linked to the positive (or negative) phase of the precipitation indices.  
 442 However, on a local scale (Fig. 8), notably in Cuba and southern Haiti, the positive effect of NAO+, corresponding to  
 443 a weakening of the subtropical anticyclone (Wallace et al., 1981; North Atlantic Oscillation, 2023) and leading to very  
 444 wet conditions in the Caribbean, particularly in the Greater Antilles (Giannini et al., 2000; Mo et al., 2005), is  
 445 associated with an increase in the number of rainy days (RR1). These results are consistent with those of Jury et al.  
 446 (2007), for whom the NAO exerts a certain influence on rainfall in the southeastern Caribbean.

447 In the case of the SOI index (fig.7), studies have already shown that ENSO influences precipitation patterns in several  
 448 regions, notably in South and North America (Ropelewski et al., 1987). However, studies (Giannini et al. 2000;  
 449 Giannini et al. 2001a; Giannini et al. 2001b; Rodriguez-Vera et al., 2019) have shown that, on an interannual scale,  
 450 ENSO is one of the most important factors influencing precipitation in the Caribbean. These results are consistent  
 451 with those of our study. The influence of ENSO was assessed on extreme precipitation indices (figure 7) using the  
 452 SOI index. For example, the positive phase of the +SOI index (sign of La Niña), characterized by abnormally cold  
 453 ocean waters in the eastern tropical Pacific, led to an increase in total annual precipitation (PRCPTOT) and heavy  
 454 precipitation (R95p) in Puerto Rico (fig. 7a, 7b). It has also led to an increase in the number of rainy days (RR1),  
 455 including the duration of wet sequences (CWD) in southern Haiti (fig. 7c, 7d), while in southeastern Cuba, it is  
 456 associated with an increase in mean rainfall intensity per rainy day (SDII) and heavy precipitation (R95p) (fig. 7b,  
 457 7e). This influence could be explained by the fact that La Nina brings wet conditions to the Caribbean ( Klotzbach,  
 458 2011).

Formatted: Font color: Auto, English (US)

Formatted: Font color: Auto, English (US)

Formatted: Font color: Auto, English (US)

Deleted: The results concerning the effect of the Atlantic Ocean, tropical Pacific, and Caribbean Sea on extreme precipitation indices show that extremes are influenced differently by the oceans and the Caribbean Sea. Moreover, at a local or regional scale, the correlation coefficients measuring trends in this influence are not statistically significant. To clarify these results, we separately discuss the effects of indices (NAO and SOI) and sea surface temperature anomalies (SST-Car, TSA) on extreme precipitation indices.

Deleted: Effect

Deleted: In this study, the effects of the Atlantic Ocean on the Greater Antilles are measured using two indices (NAO and TSA) defined over two ocean areas in two hemispheres. For the Northern Hemisphere, it has been shown that the phases (positive and negative) of the NAO index affect circulation on a Northern Hemisphere scale (Thompson et al., 2000).

Deleted: NAO index results show that the effect produced by the negative phase, corresponding to a weakening of the subtropical anticyclone (Wallace et al., 1981; North Atlantic Oscillation, 2023) and leading to very wet conditions over the Caribbean, particularly the Greater Antilles (Mo et al., 2005; Mestas-Núñez et al., 2007), is associated with a negative effect on all regional extremes

Deleted: . In other words, the NAO index evolves with extremes in the opposite direction, that is, the negative (positive) phase of the NAO is linked to the positive (negative) phase of the precipitation indices. This indicates that the extreme precipitation indices are modulated by the positive and negative phases of the North Atlantic Oscillation (NAO).

Deleted: ¶ At a local scale, the effect is observed on all extremes, except for the number of rainy days (RR1). Despite less favorable conditions for precipitation, because the +NAO index is in a positive phase, an increase is recorded on the southern coasts of Cuba and Haiti, whose coastline is the Caribbean Sea. ¶

Deleted: ¶

496

497 **5.2 Impact of sea surface temperature anomalies (TSA, SST-Car)**

498 The evolution of temperature anomalies in the South Atlantic (TSA average over 0-20S, 10E-30W) and Caribbean  
 499 Sea (SST-Car SST average 14-16N, 65-85W) presented in suppl. Fig. 3 is marked by increasing warming in the  
 500 Atlantic and Caribbean Sea over the period 1985-2015. In the Caribbean, warming has intensified over the past three  
 501 decades in both seasons (DJF and MAM) (suppl. fig.2). Thus, the +SST-Car phase in the Caribbean is associated with  
 502 an increase in all extremes at the regional scale, apart from the mean rainfall intensity per wet day (SDII) (fig. 4).  
 503 Similarly, on a local scale, considering all islands, it leads to an increase in the number of consecutive rainy days  
 504 (CWD), as well as in the number of consecutive rainy days on the island of Hispaniola (Haiti and Santo Domingo)  
 505 (fig. 6c, 6d). The increase in heavy precipitation (R95p) in Puerto Rico, southeast Cuba, and Haiti is also due to  
 506 abnormally warm conditions + SST-Car in the Caribbean Sea (fig. 6b). These results are in line with previous research  
 507 on the influence of sea surface temperature on precipitation in the Caribbean, particularly in the Greater Antilles  
 508 (Wang et al., 2007; Wang et al., 2008; Wu et al., 2011). Also, for the link between extreme precipitation and SSTs, it  
 509 has been shown that the average rainfall intensity per wet day (SDII) averaged and heavy precipitation (R95p) over  
 510 the Caribbean has a strong correlation with the warm phase of the Caribbean Sea (Peterson et al., 2002). In contrast,  
 511 the positive +TSA phase (TSA averaged over 0-20S, 10E-30W), which corresponds to warmer sea surface  
 512 temperatures (SST) in the southern tropical Atlantic (TSA), is associated with a southward shift of the ITCZ (Philander  
 513 et al., 1996) and a weakening of the southeasterly (SE) trade winds (Nobre and Shukla, 1996). This phase, which is  
 514 also associated with higher precipitation in northeastern Brazil (Utida et al., 2019), influenced precipitation indices  
 515 over the Greater Antilles, particularly in Puerto Rico and central Cuba, where it led to an increase in heavy  
 516 precipitation (R95p) (fig.5b). On the other hand, in south-eastern Cuba and north-western Haiti, this phase was  
 517 associated with an increase in rainfall intensity per wet day (SDII)(fig.6e). These results are compared with those of  
 518 the study by Utida et al. (2019), in which the influence of TSA on precipitation was assessed. The results of this study  
 519 show that the warm phase + TSA is associated with an increase in precipitation in southeastern Cuba. These findings  
 520 are consistent with my own, namely that TSA influences southeastern Cuba.

521

522 **5 Conclusion**

523 This work provides a relevant analysis of the evolution of extreme precipitation and its link with global teleconnections  
 524 over the Caribbean, particularly the Greater Antilles, over the period 1985-2015. Extreme precipitation indices  
 525 (PRCPTOT, RR1, R95p, CWD, and CDD) defined by the World Meteorological Organization Expert Team on  
 526 Climate Change Detection and Indices (ETCCDI) were calculated. Next, the links between large-scale SST oscillation  
 527 indices (NAO, SOI, TSA, and SST-CAR) and extreme precipitation indices (PRCPTOT, RR1, R95p, CWD, and CDD)  
 528 were evaluated and tested using Spearman's correlation coefficient. The results show that warming in the tropical  
 529 South Atlantic (TSA), the Caribbean Sea (mean SST 14-16N, 65-85 W), and cooling in the eastern tropical Pacific

**Deleted:** In the case of the SOI, studies have shown that the phenomena induced by phase changes (El Niño, La Niña) have a considerable impact on temperature and precipitation, particularly around the Pacific and Indian oceans (Ropelewski et al., 1987). However, the peri-Atlantic regions are also a concern, as the SOI index is associated with variability in sea surface temperatures and trade wind flows over the tropical Atlantic (Servain (1991); Zebiak (1993)). The positive phase of the +SOI index, manifested by a decrease in the zonal pressure gradient and trade wind flow, leading to persistent cooling in the central equatorial Pacific, result in a non-significant increase in all extremes on a regional scale. However, at a local scale, this positive phase, associated with cold waters in the eastern Pacific (Niña), lead to an increase in the total annual precipitation (PRCPTOT) and heavy precipitation (R95p) in Puerto Rico. It also lead to an increase in the number of rainy days (RR1), including the duration of wet sequences (CWD) in southern Haiti, as well as in the average intensity of precipitation per rainy day (SDII) and heavy precipitation (R95p) in southeastern Cuba. An increase in the duration of wet sequences (CWD) is also observed over the Saint-Dominique region. These results are in line with previous studies showing that a cold Pacific tends to favor precipitation in the Caribbean (Gimeno et al., 2011; Wu et al., 2011; Peterson et al., 2002).

**Deleted:** Effect

**Deleted:** are

**Deleted:** )

**Deleted:** lead

**Deleted:** Domingo)

**Deleted:** .

**Deleted:** The increase in heavy precipitation (R95p) in Puerto Rico, southeastern Cuba, and Haiti is also due to abnormally warm + SST-Car conditions in the Caribbean.

**Deleted:** , and on the link between sea surface temperature and extreme precipitation indices

**Deleted:** For example.

**Deleted:** I

**Deleted:** over

**Deleted:** a

**Deleted:** the positive +TSA phase (mean TSA over 0-20S, 10E-30W) is associated with warmer sea surface temperatures (SST) in the southern tropical Atlantic (TSA), leading to a southward shift of the ITCZ (Philander et al., 1996) and a weakening of the southeast (SE) trade winds (Schneider et al., 2014; Nobre and Shukla, 1996)

**Deleted:** This warm phase influences the precipitation indices over the Greater Antilles, notably the average daily precipitation intensity (SDII) over the entire region. T (... [36]

**Deleted:** These results are compared with those of a previous study (Utida et al., 2019) in which a correlation was fr (... [37]

**Formatted:** English (US)

**Deleted:** ¶

602 (Niña) have positive effects on all extreme precipitation indices. Except for the number of rainy days (RR1) and rainy  
603 episodes (CWD), for which negative correlations were observed. However, the significant effects on extremes were  
604 greatest at the island scale in the Greater Antilles. For example, in southeastern Cuba and Puerto Rico, there was an  
605 increase in heavy precipitation (R95p) and average rainfall intensity per wet day (SDII) associated with the positive  
606 phase of the indices (SOI, TSA, and SST-Car), whereas in Jamaica and northern Haiti, there were only two indices  
607 (TSA and SST-Car). The number of rainy days (RR1) and the maximum duration of consecutive rainy days (CWD)  
608 showed a significant upward trend over southern Haiti and the Dominican Republic, in line with the positive phase of  
609 the Southern Oscillation (SOI) and warming east of the Caribbean Sea surface.

Deleted: The results show that warming in the southern tropical Atlantic (TSA), the Caribbean (mean SST-Car SST 14-16N, 65-85 W), and cooling in the eastern Pacific (Niña) have positive and significant effects on extreme precipitation indices.

610 These results further improve our knowledge of the impact of certain global teleconnections on extreme precipitation  
611 in the Greater Antilles. They also highlight the most relevant teleconnection indices (SOI, SST-Car (average SST-Car  
612 SST 14-16N, 65-85 W), and TSA) to be considered as part of the impact study in the region, to limit damage to key  
613 economic sectors such as agriculture, biodiversity, health, and energy.

614

#### 615 **6 Author contribution**

616 Conceptualization: C.D, A.D, S.A; methodology: C.D, A.D, S.A; Original draft preparation: CD; review and editing:  
617 all the authors.

Deleted: ¶

Formatted: English (US)

#### 618 **7 Competing interests**

619 The authors of this paper declare that they have no conflicts of interest.

#### 621 **8 Financial supports**

622 This research was carried out with the support of the following institutions: 1) ARTS PhD grant from the Institut de  
623 Recherche pour le Développement (IRD); 2) Antenor Firmin PhD grant from the French Embassy in Haiti; 3)  
624 CARIBACT International Joint Laboratory; 4) CLIMEXHA Project (Anticipation of Extreme CLIMATE events in  
625 HAITI for sustainable development).

Formatted: English (US)

Deleted: ¶

Formatted: English (US)

#### 628 **9 Data availability**

629 The CHIRPS (Climate Hazards Group Infrared Precipitation with Stations data version 2) satellite data used in this  
630 study are available online at <https://data.chc.ucsb.edu/products/CHIRPS-2.0/>. NOAA OISST v2.1 data can also be  
631 accessed online at: (<https://www.ncdc.noaa.gov/oisst/optimum-interpolation-sea-surface-temperature-oisst-v21>).

Formatted: c-pjlv, Font: Bold, French

Formatted: Default Paragraph Font, Font: Not Bold, French

632

633

634

Deleted: ¶

Deleted: ¶

645 **Bibliography**

646 [Agudelo, P.A., Hoyos, C.D., Curry, J.A., Webster, P.J.: Probabilistic discrimination between large-scale environments](#)  
647 [of intensifying and decaying African easterly waves. \*Clim. Dyn.\* 36, 1379–1401. \[https://doi.org/10.1007/s00382-010-\]\(https://doi.org/10.1007/s00382-010-0851-x\)](#)  
648 [0851-x](#), 2011.

649

650 [Almazroui, M., Islam, M.N., Saeed, F. et al. Projected Changes in Temperature and Precipitation Over the United](#)  
651 [States, Central America, and the Caribbean in CMIP6 GCMs. \*Earth Syst Environ\* 5, 1–24,](#)  
652 [https://doi.org/10.1007/s41748-021-00199-5](#), 2021.

653

654 [An, D., Eggeling, J., Zhang, L. et al. Extreme precipitation patterns in the Asia–Pacific region and its correlation with](#)  
655 [El Niño–Southern Oscillation \(ENSO\). \*Sci Rep\* 13, 11068, <https://doi.org/10.1038/s41598-023-38317-0>, 2023.](#)

656

657 [Baez-Villanueva, O.M., Zambrano-Bigiarini, M., Ribbe, L., Nauditt, A., Giraldo-Osorio, J.D., Thinh, N.X.: Temporal](#)  
658 [and spatial evaluation of satellite rainfall estimates over different regions in Latin-America. \*Atmos. Res.\*, 213, 34–50,](#)  
659 [https://doi.org/10.1016/j.atmosres.2018.05.011](#), 2018.

660

661 [Bathelemy R., Brigode P., Boisson D., and Tric E., “Rainfall in the Greater and Lesser Antilles; Performance of five](#)  
662 [gridded datasets on a daily timescale,” \*Journal of Hydrology: Regional Studies\*, 43,101203,](#)  
663 [https://doi:10.1016/j.ejrh.2022.101203](#), 2022.

664

665 [Beharry, S.L., Clarke, R.M. & Kumarsingh, K.: Variations in extreme temperature and precipitation for a Caribbean](#)  
666 [island: Trinidad. \*Theor Appl Climatol\* 122, 783–797, <https://doi.org/10.1007/s00704-014-1330-9>, 2015.](#)

667

668 [Burgess, C.P., Taylor, M.A., Spencer, N. et al. Estimating damages from climate-related natural disasters for the](#)  
669 [Caribbean at 1.5 °C and 2 °C global warming above preindustrial levels. \*Reg Environ Change\* 18, 2297–2312,](#)  
670 [https://doi.org/10.1007/s10113-018-1423-6](#), 2018.

671

672 [Cantet, P.: Mapping the mean monthly precipitation of a small island using kriging with external drifts. \*Theor Appl\*](#)  
673 [Climatol 127, 31–44, <https://doi.org/10.1007/s00704-015-1610-z>, 2017.](#)

674

675 [Centella-Artola A, Bezanilla-Morlot A, Taylor MA, Herrera DA, Martinez-Castro D, Gouirand I, Sierra-Lorenzo M,](#)  
676 [Vichot-Llano A, Stephenson T, Fonseca C, et al. Evaluation of Sixteen Gridded Precipitation Datasets over the](#)  
677 [Caribbean Region Using Gauge Observations. \*Atmosphere\*, 11, 1334, <https://doi.org/10.3390/atmos11121334>, 2020.](#)

678

679 [Chen, Y., H. Liu, J. An, U.: Górsdorf, and F. H. Berger. : A Field Experiment on the Small-Scale Variability of](#)  
680 [Rainfall Based on a Network of Micro Rain Radars and Rain Gauges. \*J. Appl. Meteor. Climatol.\*, 54, 243–255,](#)  
681 [https://doi.org/10.1175/JAMC-D-13-0210.1](#), 2015.

682

683 [Cook, K.H., Vizy, E.K.: Hydrodynamics of the Caribbean low-level jet and its relationship to precipitation. \*J. Clim.\*](#)  
684 [23, 1477–1494, <https://doi.org/10.1175/2009JCLI3210>, 2010.](#)

685

686 [Curtis, S., and D. W. Gamble. “Regional Variations of the Caribbean Mid-Summer Drought.” \*Theoretical and Applied\*](#)  
687 [Climatology 94, 25–34, <https://doi.org/10.1007/s00704-007-0342-0>, 2008.](#)

688

689 [Daly, C., Helmer, E.H., Quiñones, M.: Mapping the climate of Puerto Rico. \*Vieques Culebra. Int. J. Clim.\* 23, 1359–](#)  
690 [1381. <https://doi.org/10.1002/joc.937>, 2003.](#)

691

**Deleted:** Agudelo, P.A., Hoyos, C.D., Curry, J.A., Webster, P.J., 2011. Probabilistic discrimination between large-scale environments of intensifying and decaying African easterly waves. *Clim. Dyn.* 36, 1379–1401.

<https://doi.org/10.1007/s00382-010-0851-x>

Almazroui, Mansour, M. Nazrul Islam, Fahad Saeed, Sajjad Saeed, Muhammad Ismail, Muhammad Azhar Ehsan, Ismaila Diallo, et al. “Projected Changes in Temperature and Precipitation Over the United States, Central America, and the Caribbean in CMIP6 GCMs.” *Earth Systems and Environment* 5, no. 1 (January 2021): 1–24.

<https://doi.org/10.1007/s41748-021-00199-5>

An, D., Eggeling, J., Zhang, L. et al. Extreme precipitation patterns in the Asia–Pacific region and its correlation with El Niño–Southern Oscillation (ENSO). *Sci Rep* 13, 11068 (2023). <https://doi.org/10.1038/s41598-023-38317-0>

Baez-Villanueva, O.M.; Zambrano-Bigiarini, M.; Ribbe, L.; Nauditt, A.; Giraldo-Osorio, J.D.; Thinh, N.X. Temporal and spatial evaluation of satellite rainfall estimates over different regions in Latin-America. *Atmos. Res.* 2018, 213, 34–50.

Bathelemy R., Brigode P., Boisson D., and Tric E., “Rainfall in the Greater and Lesser Antilles: Performance of five gridded datasets on a daily timescale,” *Journal of Hydrology: Regional Studies*, vol. 43, p. 101203, Oct. 2022. <https://doi:10.1016/j.ejrh.2022.101203>

... [38]

Formatted: English (US)

Formatted: English (US)

Formatted: English (US)

Deleted:

722 [Ríos-Cornejo, D., Penas, A., Álvarez-Esteban, R., del Río, S.: Links between teleconnection patterns and precipitation](#)  
723 [in Spain, Atmospheric Research, 156, 14-28, <https://doi.org/10.1016/j.atmosres.2014.12.012>, 2015.](#)  
724  
725  
726 [Davis, R.E., Hayden, B.P., Gay, D.A., Phillips, W.L., Jones, G.V.: The North Atlantic subtropical anticyclone. J. Clim.](#)  
727 [10, 728–744, \[https://doi.org/10.1175/1520-0442\\(1997\\)010<0728:TNASA>2.0.CO;2\]\(https://doi.org/10.1175/1520-0442\(1997\)010<0728:TNASA>2.0.CO;2\), 1997.](#)  
728  
729 [De Giorgi, A., Solarna, D., Moser, G., Tapete, D., Cigna, F., Boni, G., Rudari, R., Serpico, S.B., Pisani, A.R.,](#)  
730 [Montuori, A., et al. Monitoring the Recovery after 2016 Hurricane Matthew in Haiti via Markovian Multitemporal](#)  
731 [Region-Based Modeling. Remote Sens. 13, 3509, <https://doi.org/10.3390/rs13173509>, 2021.](#)  
732  
733 [Dookie, N., Chadee, X.T. & Clarke, R.M.: Trends in extreme temperature and precipitation indices for the Caribbean](#)  
734 [small islands: Trinidad and Tobago. Theor Appl Climatol 136, 31–44, <https://doi.org/10.1007/s00704-018-2463-z>,](#)  
735 [2019.](#)  
736  
737 [Enfield, D.B., Mestas-Nunez, A.M. and Trimble, P.J.: The Atlantic Multidecadal Oscillation and Its Relation to](#)  
738 [Rainfall and River Flows in the Continental U.S. Geophysical Research Letters, 28, 2077-2080,](#)  
739 <http://dx.doi.org/10.1029/2000GL012745>, 2001.  
740  
741 [Funk, C., Peterson, P., Landsfeld, M. et al. The climate hazards infrared precipitation with stations—a new](#)  
742 [environmental record for monitoring extremes. Sci Data 2, 150066, <https://doi.org/10.1038/sdata.2015.66>, 2015.](#)  
743  
744 [Funk, C., Verdin, A., Michaelsen, J., Peterson, P., Pedreros, D., and Husak, G.: A global satellite-assisted precipitation](#)  
745 [climatology, Earth Syst. Sci. Data\(2015a\), 7, 275–287. <https://doi.org/10.5194/essd-7-275-2015>, 2015.](#)  
746  
747 [Frich P., Alexander, L. V., Della-Marta, P., Gleason, B., Haylock, M., Klein Tank, A.M.G., and Peterson, T.: Observed](#)  
748 [Coherent Changes in Climatic Extremes during the Second Half of the Twentieth Century, Clim. Res., 19, 193 – 212,](#)  
749 <http://dx.doi.org/10.3354/cr019193>, 2002.  
750  
751 [Gauthier, T.D.: Detecting trends using Spearman's rank correlation coefficient. Environ. Forensic 2, 359–362,](#)  
752 <http://dx.doi.org/10.1006/enfo.2001.0061>, 2001.  
753  
754 [Giannini, A., Kushnir, Y., and Cane M.A. : Interannual Variability of Caribbean Rainfall, ENSO, and the Atlantic](#)  
755 [Ocean. J. Climate, 13, 297–311, \[https://doi.org/10.1175/1520-0442\\(2000\\)013<0297:IVOCRE>2.0.CO;2\]\(https://doi.org/10.1175/1520-0442\(2000\)013<0297:IVOCRE>2.0.CO;2\), 2000.](#)  
756  
757 [Giannini, A., Y. Kushnir, and M. A. Cane, Seasonality in the impact of ENSO and the North Atlantic High on](#)  
758 [Caribbean Rainfall, Phys. Chem. Earth \(B\), 28\(2\), 143–147, \[https://doi.org/10.1016/S1464-1909\\(00\\)00231-8\]\(https://doi.org/10.1016/S1464-1909\(00\)00231-8\), 2001a.](#)  
759  
760 [Giannini, A., Cane, M.A., and Kushnir Y. : Interdecadal Changes in the ENSO Teleconnection to the Caribbean](#)  
761 [Region and the North Atlantic Oscillation. J. Climate, 14, 2867–2879, \[https://doi.org/10.1175/1520-\]\(https://doi.org/10.1175/1520-0442\(2001\)014<2867:ICITET>2.0.CO;2\)  
762 \[0442\\(2001\\)014<2867:ICITET>2.0.CO;2\]\(#\), 2001b.](#)  
763  
764 [Gimeno, L., V. Magaña, and D. B. Enfield. Introduction to special section on the role of the Atlantic warm pool in the](#)  
765 [climate of the Western Hemisphere, J. Geophys. Res., 116, D00Q01, doi:10.1029/2011JD016699, 2011.](#)  
766  
767 [Griffiths, J.F. and Driscoll, J.M.: Survey of climatology. Columbus, OH: Charles Merrill,1982.](#)  
768

Formatted: English (US)

Deleted: ¶

769 [Huang, B., Liu, C., Freeman, E., Graham, G., Smith, T., and Zhang, H.: Assessment and Intercomparison of NOAA](#)  
770 [Daily Optimum Interpolation Sea Surface Temperature \(DOISST\) Version 2.1. J. Climate, 34, 7421–7441,](#)  
771 <https://doi.org/10.1175/JCLI-D-21-0001.1>, 2021.

772  
773  
774 [Hall, T.C., Sealy, A.M., Stephenson, T.S. et al. Future climate of the Caribbean from a super-high-resolution](#)  
775 [atmospheric general circulation model. Theor Appl Climatol 113, 271–287, https://doi.org/10.1007/s00704-012-0779-](#)  
776 [7](#), 2013.

777  
778 [Harris, I., Jones, P. D., Osborn, T. J. & Lister, D. H.: Mise à jour des grilles à haute résolution des observations](#)  
779 [climatiques mensuelles–l’ensemble de données CRU TS3.10. J. Climatol., 34, 623-642.https://doi-](#)  
780 [org.insu.bib.cnrs.fr/10.1002/joc.3711](#), 2014.

781  
782 [Hastenrath, S.: The intertropical convergence zone of the eastern Pacific revisited. Int. J. Climatol. 22, 347–356,](#)  
783 <https://doi.org/10.1002/joc.739>, 2002.

784  
785  
786 [Huang, B., C. Liu, V. Banzon, E. Freeman, G. Graham, B. Hankins, T. Smith, and H. Zhang. Improvements of the](#)  
787 [Daily Optimum Interpolation Sea Surface Temperature \(DOISST\) Version 2.1. J. Climate, 34, 2923–2939,](#)  
788 <https://doi.org/10.1175/JCLI-D-20-0166.1>, 2021.

789  
790 [Hurrell JW.: Decadal trends in the north atlantic oscillation: regional temperatures and precipitation. Science.,](#)  
791 [269,676-679. https://doi.org/10.1126/science.269.5224.676](#), 1995.

792  
793 [Inter-American Development Bank. Climate change and IDB: building resilience and reducing emissions; regional](#)  
794 [study: LAC small island developing states, 2014.](#)

795  
796 [IPCC. Climate Change 2007. Synthesis Report. Working Group, I, II and III contributions to the Fourth Assessment](#)  
797 [Report. http://www.ipcc.ch, 2007.](#)

798  
799 [IPCC. Climate Change 2013: The Physical Science Basis. T. F. Stocker et al., Eds., Cambridge University Press, 1535](#)  
800 [pp, 2014.](#)

801  
802 [Jones, P.D., Jónsson, T. and Wheeler, D.: Extension to the North Atlantic Oscillation using early instrumental pressure](#)  
803 [observations from Gibraltar and South-West Iceland. Int. J. Climatol. 17, 1433-1450,](#)  
804 [https://doi.org/10.1002/\(SICI\)1097-0088\(19971115\)17:13<1433::AID-JOC203>3.0.CO;2-P1997](https://doi.org/10.1002/(SICI)1097-0088(19971115)17:13<1433::AID-JOC203>3.0.CO;2-P1997), 1997.

805  
806 [Joseph, P.: La Caraïbe, données environnementales. Coordonné par Joseph P. Karthala, Paris, et Géode \(Groupe de](#)  
807 [recherche Géographie, développement, environnement de la Caraïbe\), Éditions KARTHALA. 458p, 2006.](#)

808  
809 [Jury, M., B. A. Malmgren, and A. Winter: Subregional precipitation climate of the Caribbean and relationships with](#)  
810 [ENSO and NAO. J. Geophys. Res., 112, D16107, doi:10.1029/2006JD007541](#), 2007.

811  
812 [Khadgarai, S., Kumar, V., Pradhan, P.K.: The Connection between Extreme Precipitation Variability over Monsoon](#)  
813 [Asia and Large-Scale Circulation Patterns. Atmosphere, 12, 1492. https://doi.org/10.3390/atmos12111492](#), 2021.

814  
815 [Mariani, M., Holz, A., Veblen, T. T., Williamson, G., Fletcher, M.-S., & Bowman, D. M. J. S. Climate change](#)  
816 [amplifications of climate-fire teleconnections in the Southern Hemisphere. Geophysical Research Letters, 45, 5071–](#)  
817 [5081. https://doi.org/10.1029/2018GL078294](#), 2018.

Formatted: English (US)

Deleted: ¶

818  
819 [Martens, B., Waegeman, W., Dorigo, W.A. et al. Terrestrial evaporation response to modes of climate variability. \*npj\*](#)  
820 [Clim Atmos Sci](#) 1, 43, <https://doi.org/10.1038/s41612-018-0053-5>, 2018.

821  
822 [Merchant, C.J., and Coauthors. Sea surface temperature datasets for climate applications from phase 1 of the European](#)  
823 [Space Agency Climate Change Initiative \(SST CCI\). \*Geosci. Data J.\*, 1, 179–191, <https://doi.org/10.1002/gdj3.20>,](#)  
824 [2014.](#)

825  
826 [McLean, Natalie Melissa., Stephenson, Tannecia Sydia., Taylor, Michael Alexander., and Campbell, Jayaka Danaco.](#)  
827 [“Characterization of Future Caribbean Rainfall and Temperature Extremes across Rainfall Zones.” \*Advances in\*](#)  
828 [Meteorology](#), 2015, 1–18, <https://doi.org/10.1155/2015/425987>, 2015.

829  
830  
831 [Mo, K. C., M. Chelliah, M. L. Carrera, R. W. Higgins, and W. Ebisuzaki. Atmospheric Moisture Transport over the](#)  
832 [United States and Mexico as Evaluated in the NCEP Regional Reanalysis. \*J. Hydrometeorol.\*, 6, 710–728,](#)  
833 <https://doi.org/10.1175/JHM452.1>, 2005.

834  
835  
836 [Moron, V., Frelat, R., Jean-Jeune, P.K., Gauchere, C.: Interannual and intra-annual variability of rainfall in Haiti](#)  
837 [\(1905–2005\). \*Clim. Dyn.\* 45, 915–932., <https://doi.org/10.1007/s00382-014-2326-y>, 2015.](#)

838  
839 [Naciones Unidas, Comision economica para America Latima y el Caribe, 1988, Republica Dominicana: evaluacion](#)  
840 [de los danos ocasionados por el huracan Georges, 1998, sus implicaciones para el desarrollo del pais, 91p.](#)

841  
842 [Nobre, P. and Shukla, J.: Variation of Sea Surface Temperature, Wind Stress and Rainfall over the Tropical Atlantic](#)  
843 [and South America. \*Journal of Climate\*, 9, 2464-2479, <http://dx.doi.org/10.1175/1520-0442.1996>.](#)

844  
845 [North Atlantic Oscillation, NOAA's Climate Prediction Center. Accessed December 8, 2023.](#)

846  
847 [Lewis-Beck MS. Data Analysis: An Introduction. Thousand Oaks, CA: Sage Publications, 1995.](#)

848  
849 [Love, T. B., Kumar, V., Xie, P. & Thiaw, W. A 20-year daily Africa precipitation climatology using satellite and](#)  
850 [gauge data. In Proceedings of the 84th AMS Annual Meeting, Conference on Applied Climatology, Seattle, 2004.](#)

851  
852  
853 [Peterson, T. C., C. Folland, G., Gruza., W. Hogg., A.: Mokssit, and N. Plummer, Report of the activities of the](#)  
854 [Working Group on Climate Change Detection and related rapporteurs, World Meteorol. Organ. Tech. Doc. 1071, 143](#)  
855 [pp., Comm. for Climatol., World Meteorol. Organ., Geneva, 2001.](#)

856  
857 [Peterson, T. C., et al., Recent changes in climate extremes in the Caribbean region, \*J. Geophys. Res.\*, 107, 4601,](#)  
858 <https://doi.org/10.1029/2002JD002251>, 2002.

859  
860 [Philander, S. G. H., D. Gu, D., Lambert, G., Li, T., Halpern, D., Lau, N., and Pacanowski, R.C. : Why the ITCZ Is](#)  
861 [Mostly North of the Equator. \*J. Climate\*, 9, 2958–2972, \[https://doi.org/10.1175/1520-\]\(https://doi.org/10.1175/1520-0442\(1996\)009<2958:WTHIMN>2.0.CO;2\)](#)  
862 [0442\(1996\)009<2958:WTHIMN>2.0.CO;2](#), 1996.

863  
864 [Rayner, N. A., Parker, D.E., Horton, E.B., Folland, C.K., Alexander, L.V., Rowell, D.P., Kent, E.C and Kaplan, A.:](#)  
865 [Global analyses of sea surface temperature, sea ice, and night marine air temperature since the late nineteenth century,](#)  
866 [\*J. Geophys. Res.\*, 108, 4407, <https://doi.org/10.1029/2002JD002670>, 2003.](#)

Formatted: English (US)

Formatted: English (US)

Deleted: ¶

867  
868  
869  
870  
871  
872  
873  
874  
875  
876  
877  
878  
879  
880  
881  
882  
883  
884  
885  
886  
887  
888  
889  
890  
891  
892  
893  
894  
895  
896  
897  
898  
899  
900  
901  
902  
903  
904  
905  
906  
907  
908  
909  
910  
911  
912  
913

[Reynolds, R.W., Smith, T.M., Liu, C., Chelton, D.B., Casey, K.S and M. G. Schlax. Daily high-resolution blended analyses for sea surface temperature. J. Climate, 20, 5473–5496, <https://doi.org/10.1175/2007JCLI1824.1>, 2007.](#)

[Rivera, J. A., Hinrichs, S., and Marianetti, G.: Using CHIRPS dataset to assess wet and dry conditions along the semiarid central-western Argentina. Adv. Meteor., 8413964, <https://doi.org/10.1155/2019/8413964>, 2019.](#)

[Rodrigues, M., Peña-Angulo, D., Russo, A., Zúñiga-Antón, M. & Cardil, A. Do climate teleconnections modulate wildfire-prone conditions over the Iberian Peninsula? Environ. Res. Lett. 16, 044050, <https://doi.org/10.1088/1748-9326/abe25d>, 2021.](#)

[Ropelewski C. F. et Halpert, M.S.: Global and regional scale precipitation and temperature patterns associated with El Niño–Southern Oscillation. Mon. Wea. Rev., 115, 1606-1626. \[http://dx.doi.org/10.1175/1520-0493\\(1987\\)115<1606:GARSPP>2.0.CO;2\]\(http://dx.doi.org/10.1175/1520-0493\(1987\)115<1606:GARSPP>2.0.CO;2\), 1987.](#)

Formatted: English (US)

[Saha, S., and Coauthors. The NCEP Climate Forecast System Reanalysis. Bull. Amer. Meteor. Soc., 91, 1015–1057, <https://doi.org/10.1175/2010BAMS3001.1>, 2010.](#)

[Sheskin DJ.: Handbook of Parametric and Nonparametric Statistical Procedures. 4th ed. Boca Raton, FL: Chapman & Hall/CRC; 2007.](#)

[Smith, T. M., Reynolds, R.W., Livezey, R.E., and Stokes, D.C.: Reconstruction of Historical Sea Surface Temperatures Using Empirical Orthogonal Functions. J. Climate, 9, 1403–1420. \[https://doi.org/10.1175/1520-0442\\(1996\\)009<1403:ROHSST>2.0.CO;2\]\(https://doi.org/10.1175/1520-0442\(1996\)009<1403:ROHSST>2.0.CO;2\), 1996.](#)

[Stephenson, Tannecia S., Vincent, Lucie A., Allen Theodore, Van Meerbeeck Cedric J., McLean Natalie, Peterson Thomas C., Taylor, Michael A., et al. “Changes in Extreme Temperature and Precipitation in the Caribbean Region, 1961–2010.” International Journal of Climatology 34, 2957–71, <https://doi.org/10.1002/joc.3889>, July 2014.](#)

[Khadgarai, S., Kumar, V., Pradhan, P.K.: The Connection between Extreme Precipitation Variability over Monsoon Asia and Large-Scale Circulation Patterns. Atmosphere 2021, 12, 1492. <https://doi.org/10.3390/atmos12111492>, 2021.](#)

[Klotzbach, Philip J.: “The influence of El Niño–Southern Oscillation and the Atlantic multidecadal oscillation on Caribbean tropical cyclone activity”. In: Journal of Climate 24.3, pp. 721–731, doi: 10.1175/2010JCLI3705.1, 2011.](#)

Formatted: English (US)

[Taylor, Michael A., Clarke, Leonardo A., Cantella, Abel., Bezanilla, Arnoldo., Stephenson, Tannecia S., Jones, Jhordanne., Campbell, Jayaka D., Vichot, Alejandro., and Charlery, John. “Future Caribbean Climates in a World of Rising Temperatures: The 1.5 vs 2.0 Dilemma.” Journal of Climate 31, 2907–26. <https://doi.org/10.1175/JCLI-D-17-0074.1>, April 2018.](#)

[Taylor, M. A., D. B. Enfield, and A. A.: Chen, Influence of the tropical Atlantic versus the tropical Pacific on Caribbean rainfall, J. Geophys. Res., 107\(C9\), 3127, doi:10.1029/2001JC001097, 2002.](#)

Deleted: ¶

914 [Thompson, D. W. J., and Wallace, J. M.: Annular modes in the extratropical circulation Part I: Month-to-month](#)  
915 [variability, \*J. Climate\*, 13, pp. 1000–1016, \[https://doi.org/10.1175/1520-0442\\(2000\\)013<1000:AMITEC>2.0.CO;2\]\(https://doi.org/10.1175/1520-0442\(2000\)013<1000:AMITEC>2.0.CO;2\),](#)  
916 [2000.](#)

917

918 [Thorncroft, C., Hodges, K.: African easterly wave variability and its relationship to Atlantic tropical cyclone activity,](#)  
919 [\*J. Clim.\* 14, 1166–1179, \[https://doi.org/10.1175/1520-0442\\(2001\\)014<1166:AEWVA1>2.0.CO;2\]\(https://doi.org/10.1175/1520-0442\(2001\)014<1166:AEWVA1>2.0.CO;2\), 2001.](#)

920

921 [Utida, G., Cruz, F., Etourneau, J. \*et al.\* Tropical South Atlantic influence on Northeastern Brazil precipitation and](#)  
922 [ITCZ displacement during the past 2300 years. \*Sci Rep\* 9, 1698, <https://doi.org/10.1038/s41598-018-38003-6>, 2019.](#)

923

924 [Vichot-Llano, Alejandro., Martinez-Castro, Daniel., Bezanilla-Morlot, Arnoldo., Centella-Artola, Abel., and Giorgi](#)  
925 [Filippo. “Projected Changes in Precipitation and Temperature Regimes and Extremes over the Caribbean and Central](#)  
926 [America Using a Multiparameter Ensemble of RegCM4.” \*International Journal of Climatology\* 41, 1328–50,](#)  
927 [https://doi.org/10.1002/joc.6811, 2021.](#)

928

929 [Visbeck, Martin H et al.: “The North Atlantic Oscillation: past, present, and future”. In: \*Proceedings of the National\*](#)  
930 [Academy of Sciences 98,23, pp. 12876– 12877, 2001.](#)

931

932 [Von Storch, H., Zwiers, F.C.: \*Statistical Analysis in Climate Research\*. Cambridge University Press, Cambridge 0 521](#)  
933 [45071 3,1999.](#)

934

935 [Wang, C., Enfield, D.B., Lee, S., and Landsea, C.W.: Influences of the Atlantic Warm Pool on Western Hemisphere](#)  
936 [Summer Rainfall and Atlantic Hurricanes. \*J. Climate\*, 19, 3011–3028, <https://doi.org/10.1175/JCLI3770.1.2006>,](#)

937

938 [Wang, C., S. Lee, and D. B. Enfield, Impact of the Atlantic Warm Pool on the Summer Climate of the Western](#)  
939 [Hemisphere. \*J. Climate\*, 20, 5021–5040, <https://doi.org/10.1175/JCLI4304.1>, 2007.](#)

940

941 [Wallace, J. M., and Gutzler, D.S.: Teleconnections in the Geopotential Height Field during the Northern Hemisphere](#)  
942 [Winter. \*Mon. Wea. Rev.\*, 109, 784–812, \[https://doi.org/10.1175/1520-0493\\(1981\\)109<0784: TITGHF>2.0.CO;2\]\(https://doi.org/10.1175/1520-0493\(1981\)109<0784: TITGHF>2.0.CO;2\),](#)  
943 [1981.](#)

944

945

946

947

948

949

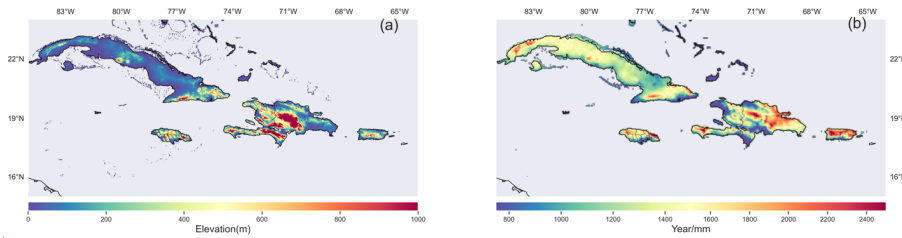
950

951

952

Formatted: English (US)

Deleted: ¶

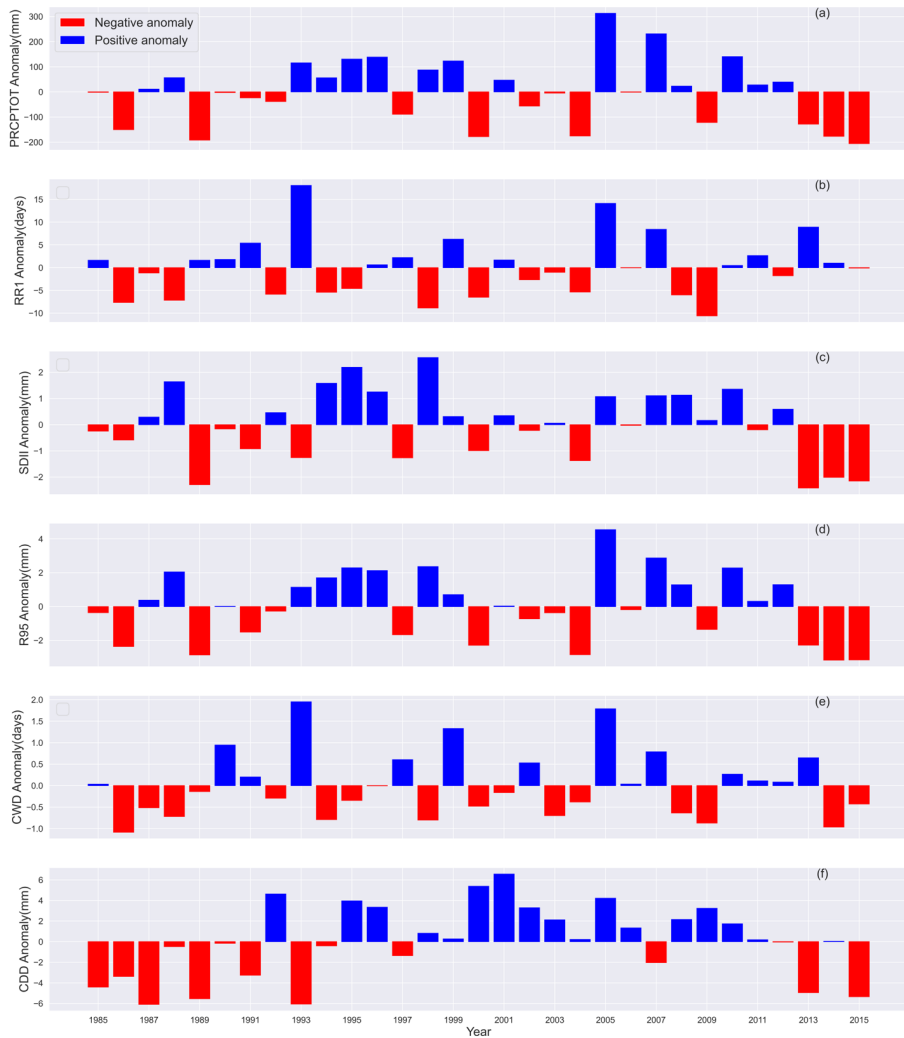


953

Figure 1. Location of study area. The figures show (a) the altitude of the four islands making up the Greater Antilles and (b) average annual rainfall.

Deleted: <object>  
 Formatted: English (US)  
 Formatted: Line spacing: Multiple 1,15 li

Deleted:



955

956 Figure 2. Interannual variability of precipitation indices in the Greater Antilles over the period 1980-2015 with (a) PRCPTOT, (b)  
 957 RR1, (c) SDII, (d) R95; (e) CWD; (f) CDD.

958

959

960

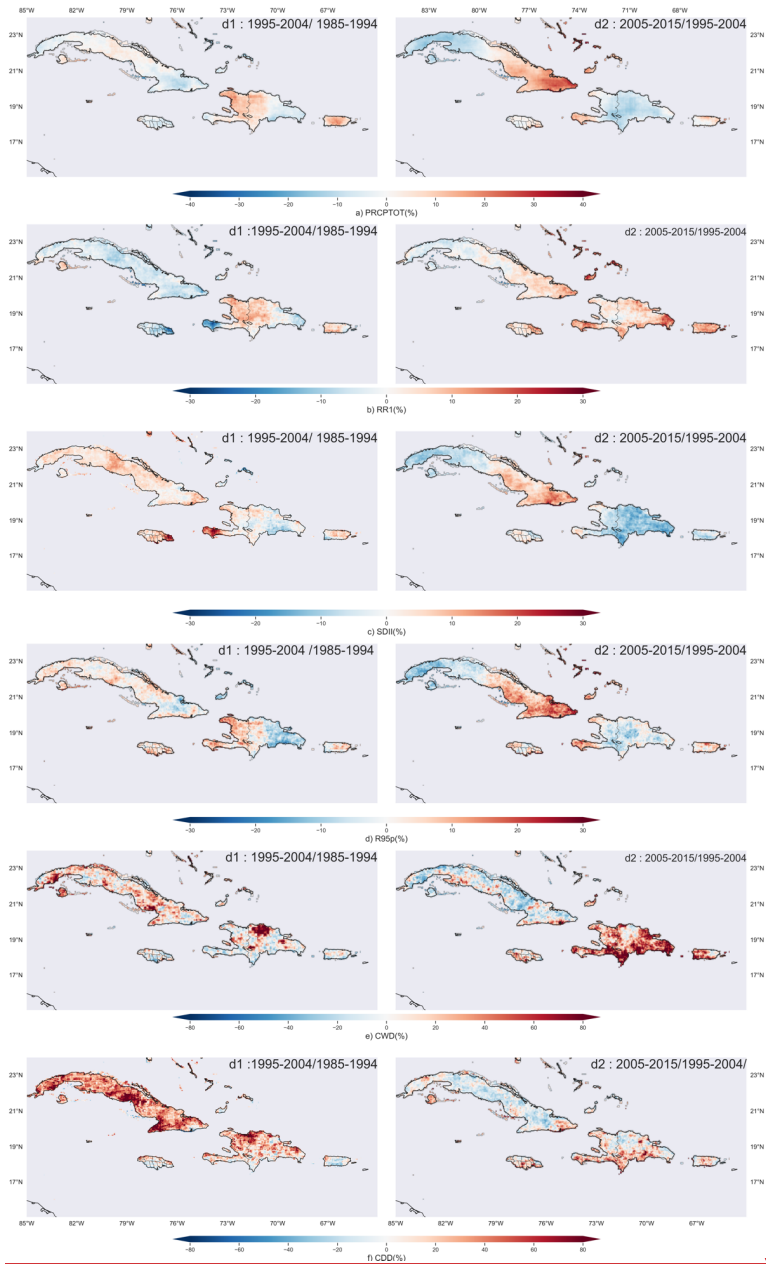
Deleted: <object>

Deleted: ¶

Deleted: <object>

Deleted: ¶

Deleted: ¶



Deleted: ¶

Formatted: Centered

Deleted: ¶

1027  
1028  
1029  
1030  
1031  
1032  
1033

Figure 3. Annual change (%) between two consecutive decades of precipitation indices over the Greater Antilles (left: 1995-2004 compared to 1985-1994; right: 2005-2015 compared to 1995-2004 right): (a) PRCPTOT, (b) RR1, (c) SDII, (d) R95p, (e) CWD (f) CDD.



1034  
1035

Figure 4. Correlation between precipitation indices and large-scale SST in the Greater Antilles (1985-2015). The values in the table are the correlation coefficients of large-scale SST with extremes. The indices on the abscissa are the precipitation extremes and those on the ordinate are the SST indices. The symbol (\*) represents a statistically significant correlation at a threshold less than or equal to 0.05.

1040  
1041  
1042  
1043  
1044  
1045  
1046  
1047

Deleted: 2015

Deleted: <object>

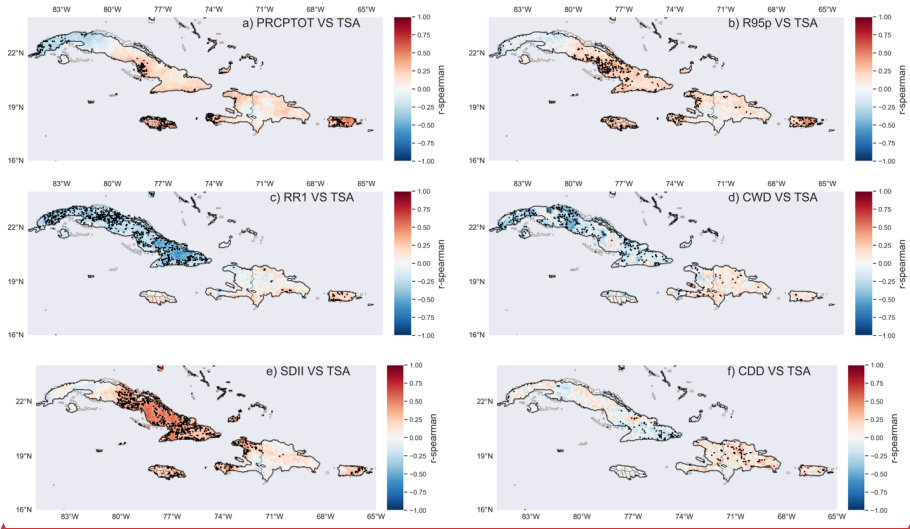
Formatted: English (US)

Formatted: Centered

Formatted: English (US)

Deleted: ¶

050  
051  
052  
053  
054



055

Figure 5. Correlation between precipitation indices and Tropical Southern Atlantic Index (TSA). The spatial correlation of extremes with TSA (SST average over 0-20S, 10E-30W) for this figure is presented in two columns; the first is realized with the indices: a) PRCPTOT Corr. TSA, b) RR1 Corr. TSA, c) SDII Corr. TSA and the second column with the indices: b) R95p Corr. TSA, d) CWD Corr. TSA, f) CDD Corr. TSA. Black dots represent areas where correlations are statistically significant at  $p \leq 0.05$ .

Formatted: English (US)

Formatted: English (US)

Formatted: English (US)

Formatted: Justified

Deleted: <

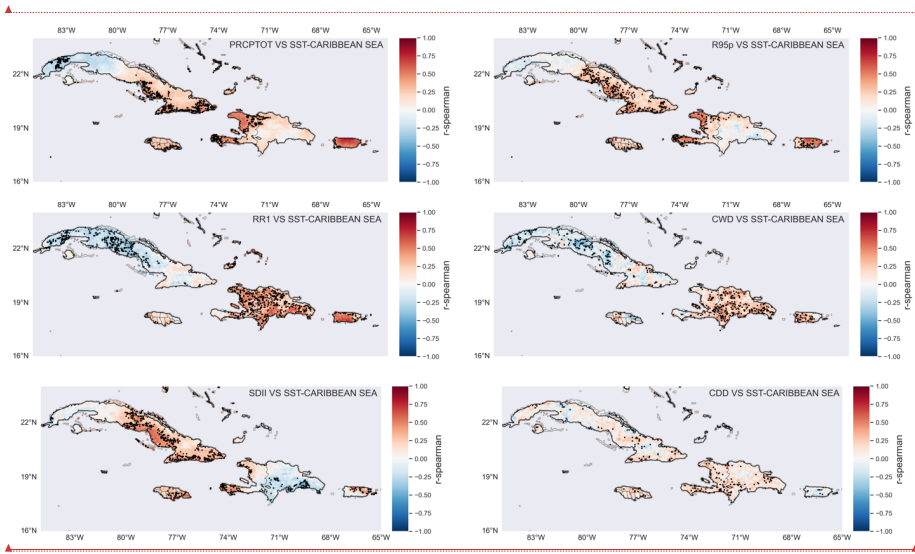
056  
057  
058  
059  
060  
061  
062  
063  
064  
065

Formatted: English (US)

Deleted: ¶  
¶

Deleted: ¶

069  
070  
071  
072  
073  
074  
075  
076  
077



078

Figure 6. Correlation between precipitation indices and Caribbean Sea surface temperature. The spatial correlation of extremes with SST-Car(SST average 14-16N, 65-85W) for this figure is presented in two columns; the first is realized with the indices: a) PRCPTOT Corr. SST-Car, b) RR1 Corr. SST-Car, c) SDII Corr. SST-Car and the second column with the indices: b) R95p Corr. SST-Car, d) CWD Corr. SST-Car, f) CDD Corr. SST-Car. Black dots represent areas where correlations are statistically significant at  $p \leq 0.05$ .

Formatted: English (US)

Formatted: English (US)

Formatted: English (US)

Deleted: <

079  
080  
081  
082  
083  
084

Deleted: <object>

Formatted: English (US)

Formatted: English (US)

Deleted: ¶

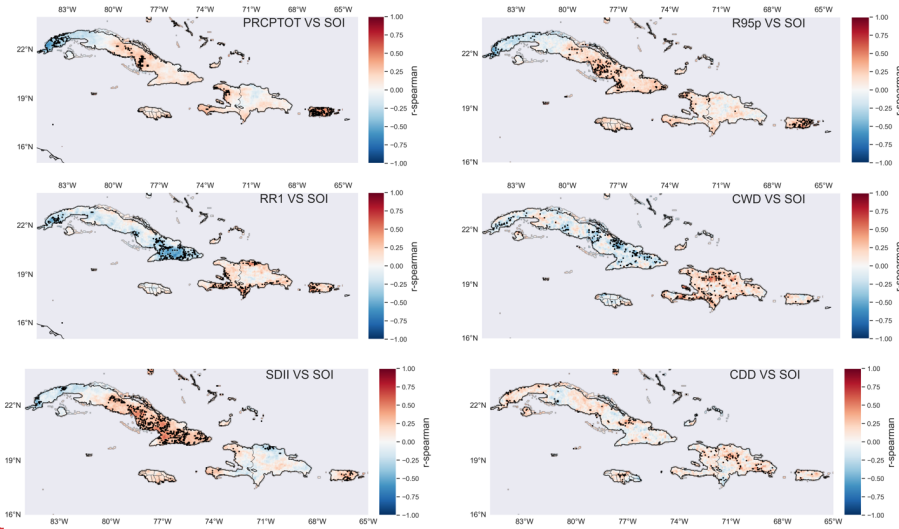
086

087

088

089

090



091

092

Figure 7. Correlation between precipitation indices and Southern Oscillation indices (SOI). The spatial correlation of extremes with SOI for this figure is presented in two columns; the first is realized with the indices: a) PRCPTOT Corr. SOI, b) RR1 Corr. SOI, c) SDII Corr. SOI and the second column with the indices: b) R95p Corr. SOI, d) CWD Corr. SOI, f) CDD Corr. SOI. Black dots represent areas where correlations are statistically significant at  $p \leq 0.05$ .

093

094

095

096

097

098

099

100

101

Formatted: English (US)

Deleted: ¶

Deleted: <object>

Formatted: English (US)

Formatted: English (US)

Formatted: Justified

Formatted: English (US)

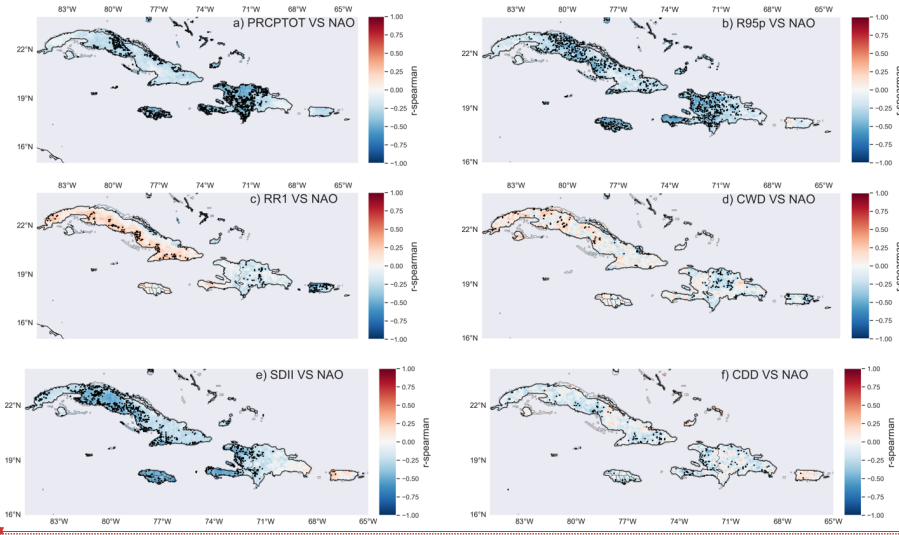
Formatted: English (US)

Deleted: <

Formatted: Font: 9 pt

Deleted: ¶

106  
107  
108  
109



110  
111

Figure 8. Correlation between precipitation indices and North Atlantic Oscillation Indices (NAO). The spatial correlation of extremes with NAO for this figure is presented in two columns; the first is realized with the indices: a) PRCPTOT Corr. NAO, b) RR1 Corr. NAO, c) SDII Corr. NAO and the second column with the indices: b) R95p Corr. NAO, d) CWD Corr. NAO, f) CDD Corr. NAO. Black dots represent areas where correlations are statistically significant at  $p \leq 0.05$ .

112  
113  
114

Formatted: English (US)

Deleted: ¶

Deleted: <object>

Formatted: English (US)

Formatted: English (US)

Formatted: Centered

Formatted: English (US)

Deleted: <

Formatted: Font: 9 pt

Formatted: English (US)

Deleted: ¶

119  
120  
121  
122

Table 1 Definition of extreme precipitation indices used in this study.

ID	Index Name	Indices definition	Units
RR1	Total wet days index	Number of days with precipitation amount $\geq 1$ mm. Let $RR_{ij}$ be the day daily precipitation amount on day $i$ in period $j$ . Count the number of days where: $RR_{ij} \geq 1$ mm.	days
PRCPTOT	Annual total precipitation on a wet day	Annual total precipitation on wet days. Let $RR_{ij}$ be the daily precipitation amount on day $i$ in period $j$ . If $I$ represent the number of days in $I$ , then: $PRCPTOT_I = \sum_{i=1}^I RR_{ij}$	mm
SDII	Simple daily rainfall intensity index	Simple daily rainfall intensity index: Let $RR_{ij}$ be the daily precipitation amount on a wet day, with $RR_{ij} > 1$ mm in period $j$ . If $W$ represents the number of wet days in $j$ , then: $SDII_j = \frac{\sum_{w=1}^W RR_{wj}}{W}$	mm/day
CWD	Consecutive wet days	Maximum number of consecutive days wet days. Let $RR_{ij}$ be the daily day precipitation amount on day $i$ in period $j$ . Count the largest number of consecutive days where: $RR_{ij} \geq 1$ mm.	days
CDD	Consecutive dry days	Maximum number of consecutive dry days. Let $RR_{ij}$ be the daily day precipitation amount on day $i$ in period $j$ . Count the largest number of consecutive days where: $RR_{ij} < 1$ mm.	days
R95p	Very wet days	The 95th percentile of daily precipitation events is the value above mm/day which 5% of the daily precipitation events are found.	mm/day

- Formatted: Font: 10 pt, Not Bold
- Deleted: P
- Formatted: Font: Not Bold, English (US)
- Formatted: Font: Not Bold
- Formatted: Font: Not Bold
- Formatted: Font: Not Bold, English (US)
- Formatted: Font: 10 pt
- Formatted: Justified
- Deleted: W
- Formatted: Font: 10 pt
- Deleted: Number of wet days  $\geq 1$ mm
- Deleted: rainfall
- Deleted: wet day
- Formatted: Justified
- Formatted: Justified
- Formatted: Justified
- Deleted: with daily rainfall  $\geq 1$ mm
- Formatted: Justified
- Deleted: days with daily rainfall  $< 1$ mm
- Formatted: English (US)
- Deleted: M
- Deleted: .
- Deleted: Annual total PRCP when  $RR > 95$ th percentile.
- Formatted: English (US)

123  
124  
1125

Deleted: ¶

**Page 6: [1] Deleted** Carlo DESTOUCHES 9/26/24 10:09:00 AM

▼ .....  
▲ .....

**Page 6: [2] Deleted** Carlo DESTOUCHES 10/6/24 12:55:00 PM

▼ .....  
▲ .....

**Page 6: [3] Formatted** Carlo DESTOUCHES 10/12/24 10:50:00 AM

c-pjlv, Font: 10 pt, Font color: Auto, French

**Page 6: [4] Formatted** Carlo DESTOUCHES 10/12/24 10:50:00 AM

c-pjlv, Font: 10 pt, French

**Page 6: [5] Deleted** Carlo DESTOUCHES 9/26/24 1:35:00 PM

▼ .....  
▲ .....

**Page 6: [6] Formatted** Carlo DESTOUCHES 10/12/24 10:50:00 AM

Font: 10 pt

**Page 6: [7] Formatted** Carlo DESTOUCHES 10/12/24 10:50:00 AM

English (US)

**Page 6: [8] Formatted** Carlo DESTOUCHES 10/12/24 10:50:00 AM

English (US)

**Page 6: [9] Formatted** Carlo DESTOUCHES 10/12/24 10:50:00 AM

English (US)

**Page 6: [10] Formatted** Carlo DESTOUCHES 10/12/24 10:50:00 AM

English (US)

**Page 6: [11] Formatted** Carlo DESTOUCHES 10/12/24 10:50:00 AM

English (US)

**Page 6: [12] Formatted** Carlo DESTOUCHES 10/12/24 10:50:00 AM

English (US)

▲  
**Page 6: [13] Formatted** Carlo DESTOUCHES 10/12/24 10:50:00 AM

English (US)

▲  
**Page 6: [14] Formatted** Carlo DESTOUCHES 10/12/24 10:50:00 AM

English (US)

▲  
**Page 6: [15] Formatted** Carlo DESTOUCHES 10/12/24 10:50:00 AM

English (US)

▲  
**Page 6: [16] Formatted** Carlo DESTOUCHES 10/12/24 10:50:00 AM

English (US)

▲  
**Page 6: [17] Formatted** Carlo DESTOUCHES 10/12/24 10:50:00 AM

English (US)

▲  
**Page 6: [18] Formatted** Carlo DESTOUCHES 10/12/24 10:50:00 AM

English (US)

▲  
**Page 6: [19] Formatted** Carlo DESTOUCHES 10/12/24 10:50:00 AM

English (US)

▲  
**Page 6: [20] Formatted** Carlo DESTOUCHES 10/12/24 10:50:00 AM

English (US)

▲  
**Page 6: [21] Formatted** Carlo DESTOUCHES 10/12/24 10:50:00 AM

English (US)

▲  
**Page 6: [22] Formatted** Carlo DESTOUCHES 10/12/24 10:50:00 AM

English (US)

▲  
**Page 6: [23] Formatted** Carlo DESTOUCHES 10/12/24 10:50:00 AM

English (US)

▲  
**Page 6: [24] Formatted** Carlo DESTOUCHES 10/12/24 10:50:00 AM

English (US)

▲  
**Page 6: [25] Formatted** Carlo DESTOUCHES 10/12/24 10:50:00 AM

English (US)

▲  
**Page 6: [26] Formatted** Carlo DESTOUCHES 10/12/24 10:50:00 AM

Subscript

▲ **Page 6: [27] Formatted** Carlo DESTOUCHES 10/12/24 10:50:00 AM

Subscript

▲ **Page 6: [28] Formatted** Carlo DESTOUCHES 10/12/24 10:50:00 AM

English (US)

▲ **Page 6: [29] Formatted** Carlo DESTOUCHES 10/12/24 10:50:00 AM

English (US)

▲ **Page 6: [30] Formatted** Carlo DESTOUCHES 10/12/24 10:50:00 AM

English (US)

▲ **Page 6: [31] Formatted** Carlo DESTOUCHES 10/12/24 10:50:00 AM

English (US)

▲ **Page 6: [32] Formatted** Carlo DESTOUCHES 10/12/24 10:50:00 AM

English (US)

▲ **Page 6: [33] Formatted** Carlo DESTOUCHES 9/26/24 11:55:00 AM

Normal, Left, Line spacing: Multiple 1,15 li

▲ **Page 6: [34] Formatted** Carlo DESTOUCHES 10/12/24 10:50:00 AM

Font: Not Bold

▲ **Page 6: [35] Formatted** Carlo DESTOUCHES 10/2/24 11:09:00 AM

Justified, Line spacing: 1,5 lines

▲ **Page 10: [36] Deleted** Carlo DESTOUCHES 10/12/24 10:47:00 AM

▼

▲ **Page 10: [37] Deleted** Carlo DESTOUCHES 10/12/24 11:30:00 AM

▼

▲ **Page 12: [38] Deleted** Carlo DESTOUCHES 9/18/24 9:41:00 PM

▲